



Triple diagram models for prediction of suspended solid concentration in Lake Okeechobee, Florida

Abdüselam Altunkaynak^{a,b,*}, Keh-Han Wang^b

^a Faculty of Civil Engineering, Hydraulics, Division, Istanbul Technical Univ., Maslak 34469, Istanbul, Turkey

^b Department of Civil and Environmental Engineering, University of Houston, 4800 Calhoun, Houston, TX 77204-4003, United States

ARTICLE INFO

Article history:

Received 26 November 2009

Received in revised form 10 March 2010

Accepted 29 March 2010

This manuscript was handled by Dr. A. Bardossy, Editor-in-Chief, with the assistance of Ercan Kahya, Associate Editor

Keywords:

Contour map

Prediction

Kriging optimum interpolation technique

Lake Okeechobee

Sediment/water interaction

Model

SUMMARY

Lake Okeechobee in Florida is a major component of the greater Everglades hydrologic system and provides a number of valuable uses to society and nature, such as water supply, navigation, wildlife habitat, and fishery. Suspended solid concentration (SSC) affects directly the lake's conditions for some of these applications. Therefore, accurate prediction of SSC can enhance the management of the water quality and the long-term protection of Lake Okeechobee. Extensive data, including wind speed, flow velocity, flow direction and SSC, have been collected. Models for predicting suspended solid concentration based on 10 different scenarios are developed using these measurements. Data are divided into two groups as training and testing for the construction of the models. SSC is predicted by the Kriging interpolation technique. Criteria of mean relative error, root mean squared error and coefficient of efficiency (CE) are used to determine the prediction errors of the developed models. In general, mean relative error is below 7% and coefficient of efficiency stays above 0.92 for the models presented. Graphs, results, and interpretations are given in detail in this paper.

© 2010 Elsevier B.V. All rights reserved.

1. Introduction

Lake Okeechobee is one of the most important water bodies in the state of Florida for the use of different purposes such as, water supply, navigation, wildlife habitat and commercial fishery. The lake, located in south-central Florida, covers a surface area of 1730 km² with an average depth of 2.7 m (South Florida Water Management District (SFWMD), 2007). Considering its huge storage capacity as the largest lake in the southeastern United States, Lake Okeechobee also serves important hydrologic and ecologic roles for the region of great Everglades in Florida.

Wind has a dominant effect on the motion and mixing of water in shallow water bodies. In Lake Okeechobee flow circulation, free-surface oscillation, and transportation of the sediments are attributable to wind blowing over the lake (Wang et al., 2003). A modeling study of wind induced sediment resuspension in a shallow estuary by Liu and Huang (2009) also confirmed the strong correlation between wind and the transport of suspended sediments. The bottom sediments in Lake Okeechobee contain a large area of semi-fluid mud. Resuspended sediment is a major concern

in Lake Okeechobee. Sediment resuspension causes greater turbidity and reducing light penetration through the water column. It is also noticeable that the internal phosphorus loads associated with resuspended sediments are approximately the same order of magnitude as the external loads (Reddy 1991). By examining the phosphorus budgets of Lake Okeechobee, for around 10 years span of 1990th, the phosphorus has accumulated in the sediments at the rate of 303 metric tons per year (Reedy et al. 2002). Therefore, over the decades through excessive phosphorus (P) loading and accumulation of fine sediments, there is an increasing concern that the increase of suspended sediments may be impacting the water quality of the lake.

An extensive field study on Lake Okeechobee has been carried out by Wang et al. (2003) to collect time varying hydrodynamic data including three-dimensional flow velocities and suspended solid concentrations. The effects of wind and flow velocities on transporting SSC were analyzed statistically. Currently, a Lake Okeechobee Environmental Model (LOEM) has been applied to predict water circulation patterns and suspended solid concentration (SSC) (Jin et al., 2002; Jin and Ji, 2004). However, it would be interesting and practical to establish other predictive models that can provide more effective and accurate estimation on SSC for the impact study of the Lake Okeechobee.

The Triple Diagram Model (TDM), firstly proposed by Altunkaynak and his colleagues in 2003, concurrently shows the variation of

* Corresponding author at: Department of Civil and Environmental Engineering, University of Houston, 4800 Calhoun, Houston, TX 77204-4003, United States.

E-mail addresses: altunkay@itu.edu.tr, aaltunka@mail.uh.edu (A. Altunkaynak), khwang@uh.edu (K.-H. Wang).

three variables and can be used for predictions (Altunkaynak et al., 2003; Şen et al., 2004). Also, plots obtained by this technique facilitate the procedure of making useful explanations of the influencing trend among variables. To establish the TDM, three variables, including two affecting variables, and one dependent variable, are required. In this study, 10 TDMs are developed with the application of the constructed contour maps of three variables to identify and relate the effects of wind speed (WS), surface flow velocity (FV), and flow direction (FD) to SSC and the classical Kriging technique, or the so called geostatistical approach, (Matheron, 1963) to determine the time variation of SSC at a station in Lake Okeechobee.

2. Kriging approach

The principal of the Kriging (optimum interpolation) approach is to establish a valid variogram model that can interpret and characterize the structural relationships of natural phenomenon. In other words, the variogram model can be used as a simple and reliable statistical tool to interpret the regional behaviour of a random field. The Kriging method (Krige, 1951) has been adopted for applications in various areas, such as earth sciences (Journel and Huijbregts, 1978; Isaaks and Srivastava, 1989; Cressie, 1993), mining (Matias et al., 2004), tunnels (Öztürk and Nasuf, 2002), ocean engineering (Altunkaynak, 2005; Ozger and Sen, 2007) and hydrology (Altunkaynak, 2009; Altunkaynak et al., 2003; Şen et al., 2004). In this study, a series of SSC related contour maps are prepared by using the geostatistical approach for the development of prediction models for SSC in the water column of the Lake Okeechobee.

One of the major principles of the geostatistical applications is to describe the behaviour of a natural phenomenon relying on two different variables. For the present Lake Okeechobee study, variables such as wind speed, flow velocity, and flow direction can be paired as two input location variables for the prediction of SSC as regional variable (ReV). For example, SSC contour maps can be constructed with the variables of wind speed and flow velocity using Kriging approach. Other contour maps with selection of two other input variables can also be obtained. Overall, this mapping technique is adopted to facilitate the understanding of the alteration of current SSC with the effects of wind speed, flow velocity, flow direction, and previous SSC. It is also applied to show the relationships between the surface SSC with the middle-layer SSC or the bottom-layer SSC.

Regional dependency between scattered points can be defined by the following equation (Matheron, 1963; Journel and Huijbregts, 1978; Isaaks and Srivastava, 1989; Şen 1989),

$$\gamma(d) = \frac{1}{2N(d)} \sum_{i=1}^{N(d)} [C(x+d) - C(x)]^2 \quad (1)$$

This expression is called semivariogram (SV) function. Here, $\gamma(d)$ = SV function; $N(d)$ = number of pairs of two variables for distance d ; $C(x)$ = magnitude of the regional variable; and $C(x+d)$ = magnitude of the regional variable that is away from the $C(x)$ by a distance d . For example, when the wind speed and flow velocity are considered as the independent variables and the SSC as the dependent variable, the distances are calculated between data points formed by the wind speed and flow velocity. Generally, a geostatistical study covers two steps: (i) obtaining semivariogram and (ii) solving the prediction problem using the Kriging. The fundamental procedure of a Kriging system is to minimize the error variance (Isaaks and Srivastava, 1989; Subyani 1997; Altunkaynak et al. 2003; Şen et al., 2004). The following equation can be used for the SSC prediction at any point of the contour map,

$$C(x_o) = \sum_{i=1}^N w_i C(x_i) \quad (2)$$

Here, $C(x_o)$ = magnitude of the SSC at any prediction point x_o ; $C(x_i)$ = SSC measurements at point i ; and w_i = weighting coefficients that can be determined by solving the following system of equations constructed from the semivariogram function (Isaaks and Srivastava, 1989; Subyani, 1997)

$$\begin{bmatrix} w_1 \\ w_2 \\ \cdot \\ w_n \\ \mu \end{bmatrix} = \begin{bmatrix} \gamma_{11} & \gamma_{12} & \cdot & \gamma_{1n} & 1 \\ \gamma_{21} & \gamma_{22} & \cdot & \gamma_{2n} & 1 \\ \cdot & \cdot & \cdot & \cdot & \cdot \\ \gamma_{n1} & \gamma_{n2} & \cdot & \gamma_{nn} & 1 \\ 1 & 1 & 1 & 1 & 0 \end{bmatrix}^{-1} \begin{bmatrix} \gamma_{1o} \\ \gamma_{2o} \\ \cdot \\ \gamma_{no} \\ 1 \end{bmatrix} \quad (3)$$

Here γ_{ij} = values of semivariogram between two points, namely, i and j ; γ_{io} = values of semivariogram between point i and the prediction point o ; and μ = Lagrange parameter. Therefore, the weighting matrix can be obtained from two variables (e.g. a combination of two variables selected from wind speed, flow velocity, flow direction, and SSC at previous time level) by applying various scenarios of the variables for the development of predictive models for estimating the surface-layer SSC or SSC at middle or bottom layer.

3. Study area and sources of data

Lake Okeechobee (Fig. 1) is located in south-central Florida and covers nearly 1730 km² with an average depth of only 2.7 m. Lake Okeechobee is the “liquid heart” of South Florida. It is a large, shallow, eutrophic lake. Its maximum water storage capacity is about 3.97 billion m³. After Lake Michigan, Lake Okeechobee is the second-largest freshwater lake in the continental United States and its drainage basin covers more than 11,914 km² (James et al., 1995; Wang et al. 2003). The main sources of water to the lake are rainfall and the Kissimmee River. Lake Okeechobee’s major outflows are the westward flowing Caloosahatchee River, the St. Lucie Canal to the east, and the agricultural canals that bring water southward through the Everglades agricultural area and into the developed areas of south Florida’s east coast. A large amount of water is also lost to the atmosphere through evapotranspiration.

The sediments in Lake Okeechobee have a high organic content. The bottom sediments include a large area of more than 10-cm thick fluid mud. This sediment is easily entrained and transported into the water column. Therefore, resuspended sediments are a common problem in Lake Okeechobee. Sediment resuspension (or the turbidity) results in the reduction of light penetration through the water column. This leads to the decline of submerged plant beds. As submerged plants compete with water column algae (phytoplankton) for nutrients and help to stabilize sediments, plant losses can further accelerate deterioration of water quality. Sediment resuspension can also cause the increased inputs of phosphorus to the water column (SFWMD, 2007).

Recently, to enhance the development and calibration of predictive models for SSC, Wang et al. (2003) conducted field measurements in Lake Okeechobee to collect continuous data describing three-dimensional velocity distribution and SSCs from January 18 to March 5, 2000. A complete data set including the velocity distribution and SSCs at surface layer (302 cm from the bottom), middle layer (145 cm from the bottom), and bottom layer (95 cm from the bottom) were recorded at the interval of 15 min at Station L006 (Fig. 1). Detailed description of the field measurements can be found in Wang (2000a,b) and Wang et al. (2003). The wind data at the interval of 15 min were collected by the SFWMD. In this study, the gathered wind speed, fluid velocity at the surface layer,

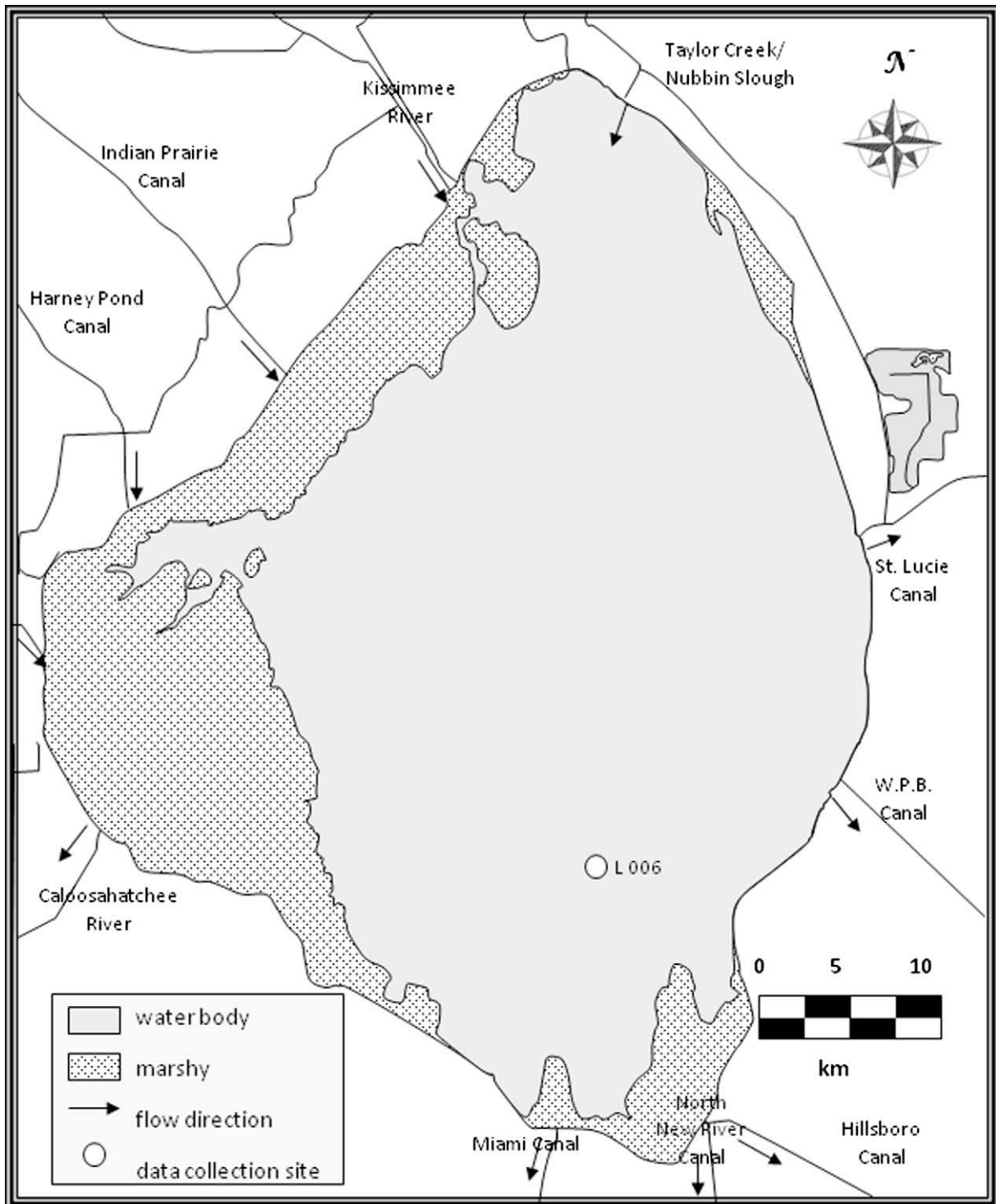


Fig. 1. Lake Okeechobee and the location of station L006. The map of Lake Okeechobee was generated by using two discrete successive orthorectified LANDSAT-7 images taken in 1st of September 2002.

fluid velocity direction (or flow direction), and SSC data at station L006 are adopted for the development of triple diagram models for the prediction of suspended solid concentration.

4. Results and discussion

As described above, the level of SSC plays an important role in affecting the water quality of Lake Okeechobee, it is necessary to

develop predictive models to estimate the SSC accurately. In this study, one of the focuses is to develop models for predicting the surface SSC using the related surface hydrodynamic data as the inputs. Development of other models for predicting the SSCs at the middle and bottom layers is also conducted. Contour maps as shown in Fig. 2 from the Kriging approach using the data collected at station L006 are obtained to determine and to interpret how the current surface SSC changes with the previous surface SSC, wind speed, surface flow velocity, or flow direction for the development

of predictive models. Presented in Figs. 3 and 4 are the contour maps used to develop models that predict the values of middle-layer SSC and bottom-layer SSC from the inputs of surface SSC. As we know obtaining the measurements at the surface level are

generally easier than the middle or bottom level. Therefore, in principle, only limited efforts are needed to collect the data of surface SSC as the SSC at the other layers can be predicted from the calibrated models. In this study, we establish and test 10 TDMs

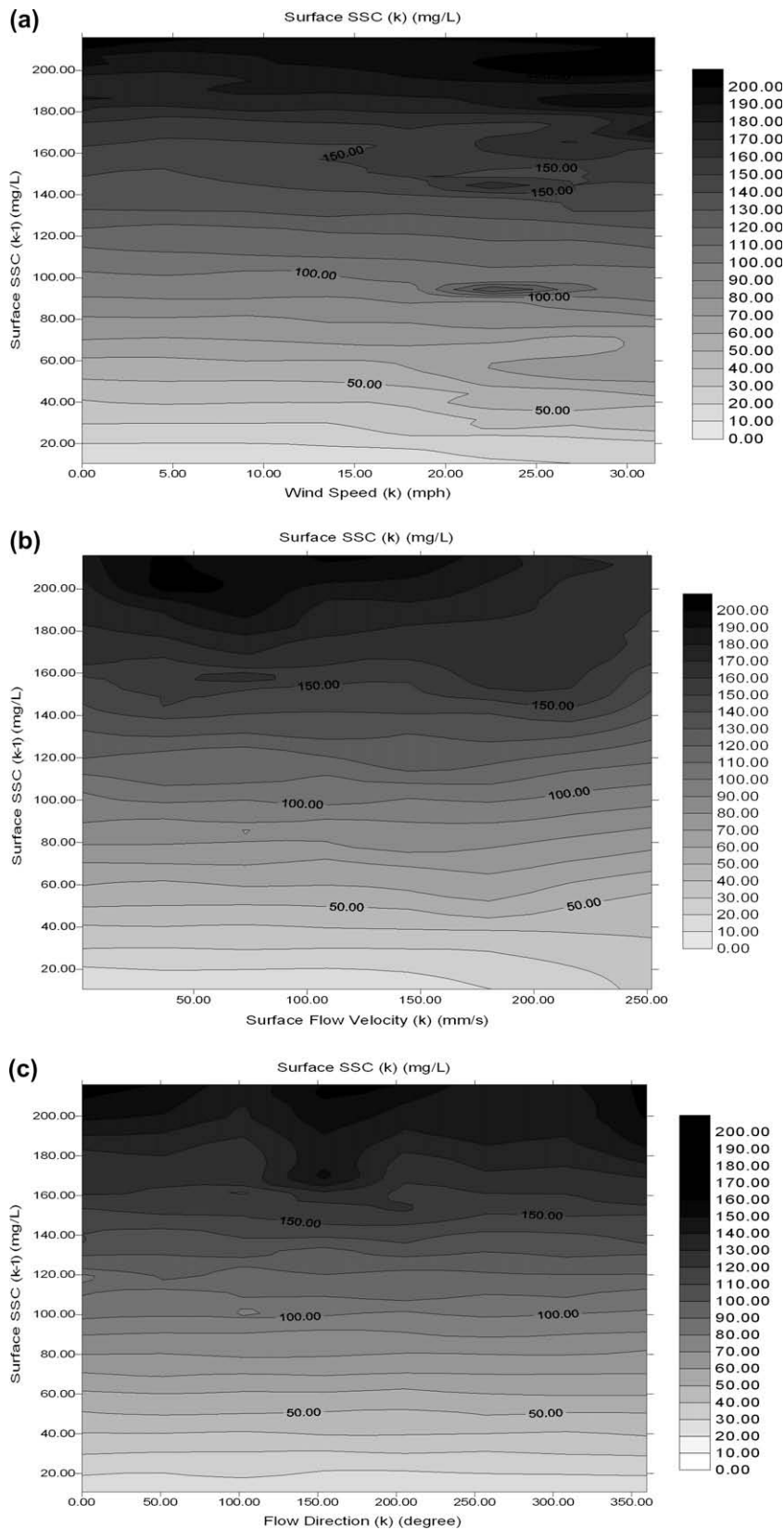


Fig. 2. Surface suspended solid concentration (SSC) contour maps using: (a) Model 1, (b) Model 2, (c) Model 3.

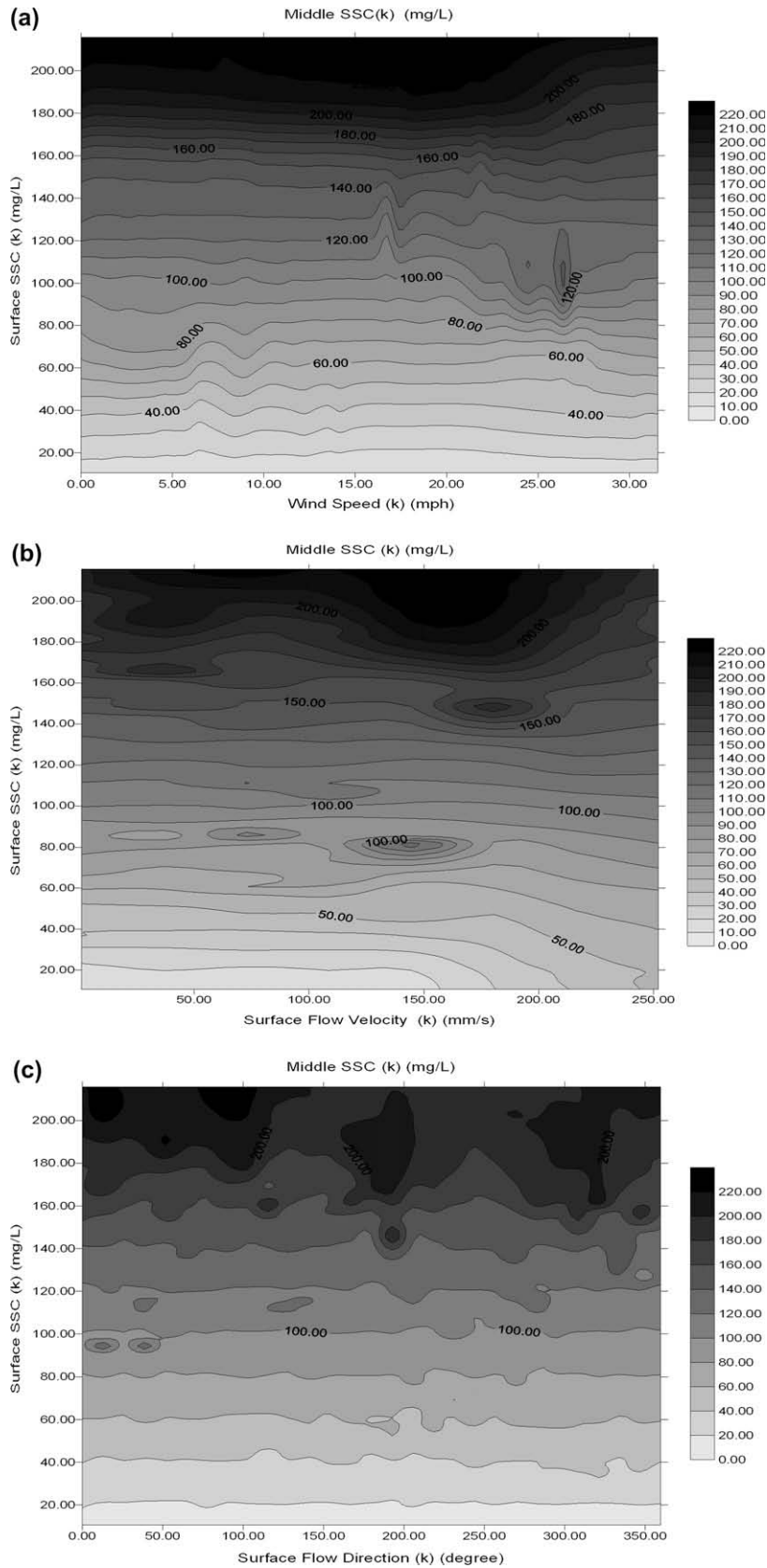


Fig. 3. Middle-layer suspended solid concentration (SSC) contour maps using: (a) Model 4, (b) Model 5, (c) Model 6.

for predicting the current SSC at L06 based on the current (time step k) or previous (time step $k - 1$) data of affecting variables. Data are divided into two groups; one group with 3500 data points

is for the training (or calibration) and the other group with the remaining 1000 data points is for the prediction (testing or validation). Contour maps of Models 1–10 are given in Figs. 2–5. Details

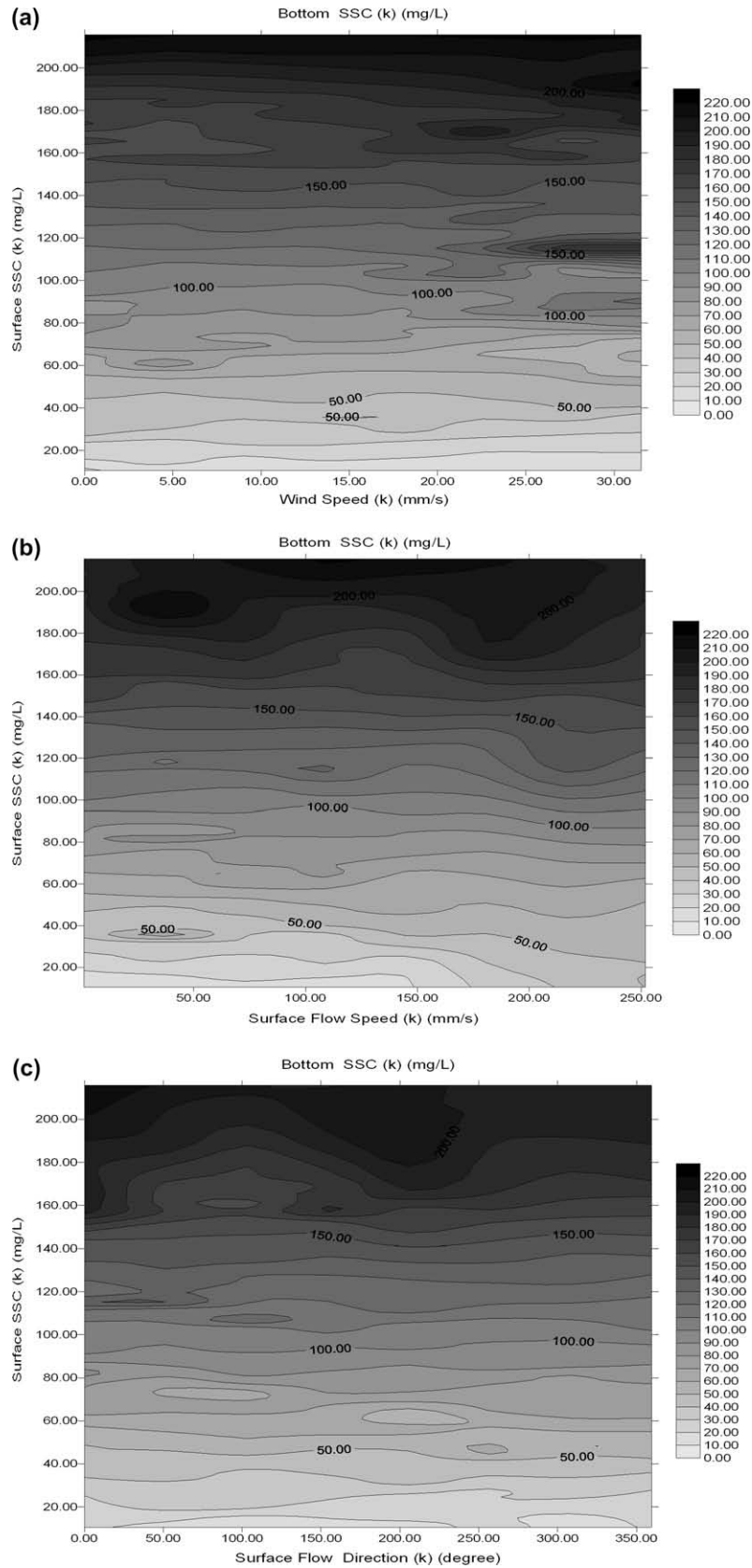


Fig. 4. Bottom-layer suspended solid concentration (SSC) contour maps using: (a) Model 7, (b) Model 8, (c) Model 9.

of these models with the selections of the input and output variables as well as the analyzed errors are summarized in Table 1.

Considering the important effect of previous surface SSC on the prediction of current surface SSC (at k time level), the basic models

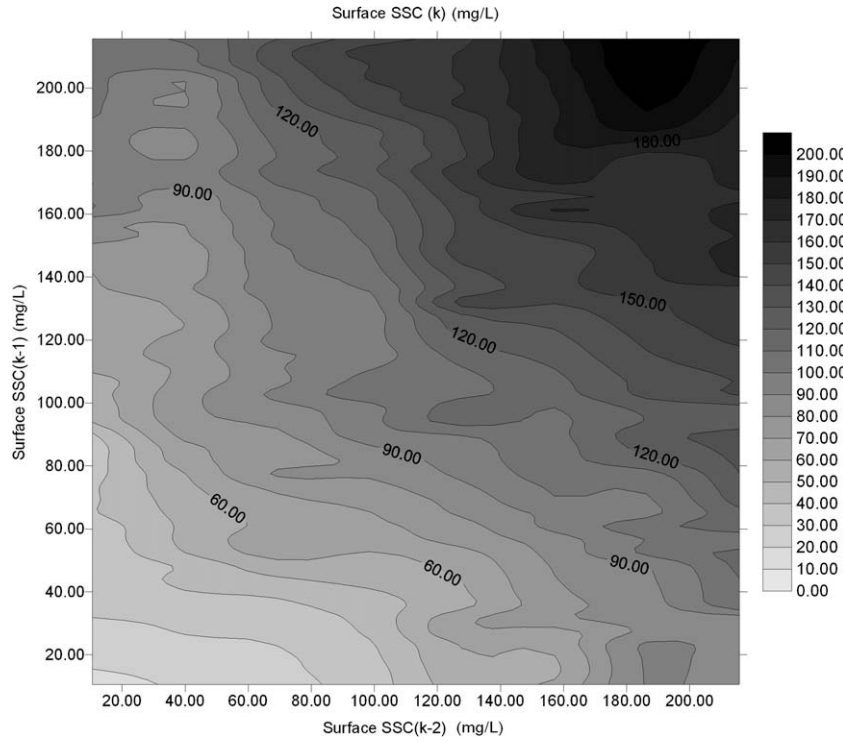


Fig. 5. Surface suspended solid concentration (SSC) contour maps using Model 10.

Table 1
Various scenarios to predict suspended solid concentration (SSC).

Model number	Inputs	Output	Mean relative errors (%)	Root mean squared errors (mg/L)	Coefficient of efficiency
1	Surface WS(k) SSC(k-1)	Surface SSC(k)	3.03	3.01	0.98
2	Surface FV(k) SSC(k-1)	Surface SSC(k)	3.21	3.07	0.98
3	Surface FD(k) SSC(k-1)	Surface SSC(k)	3.27	3.14	0.98
4	Surface WS(k) SSC(k)	Middle SSC(k)	4.97	4.14	0.96
5	Surface FV(k) SSC(k)	Middle SSC(k)	5.94	4.64	0.95
6	Surface FD(k) SSC(k)	Middle SSC(k)	5.86	4.60	0.95
7	Surface WS(k) SSC(k)	Bottom SSC(k)	6.25	5.48	0.93
8	Surface FV(k) SSC(k)	Bottom SSC(k)	6.76	5.75	0.92
9	Surface FD(k) SSC(k)	Bottom SSC(k)	6.55	5.56	0.93
10	Surface SSC(k-2) SSC(k-1)	Surface SSC(k)	3.73	3.46	0.97

Coefficient of efficiency(CE) = $1 - \frac{\sum_{i=1}^N (x_{0i} - x_{pi})^2}{\sum_{i=1}^N (x_{0i} - \bar{x})^2}$.
 x_{0i} : measurement; x_{pi} : prediction; \bar{x} : average of measurements.

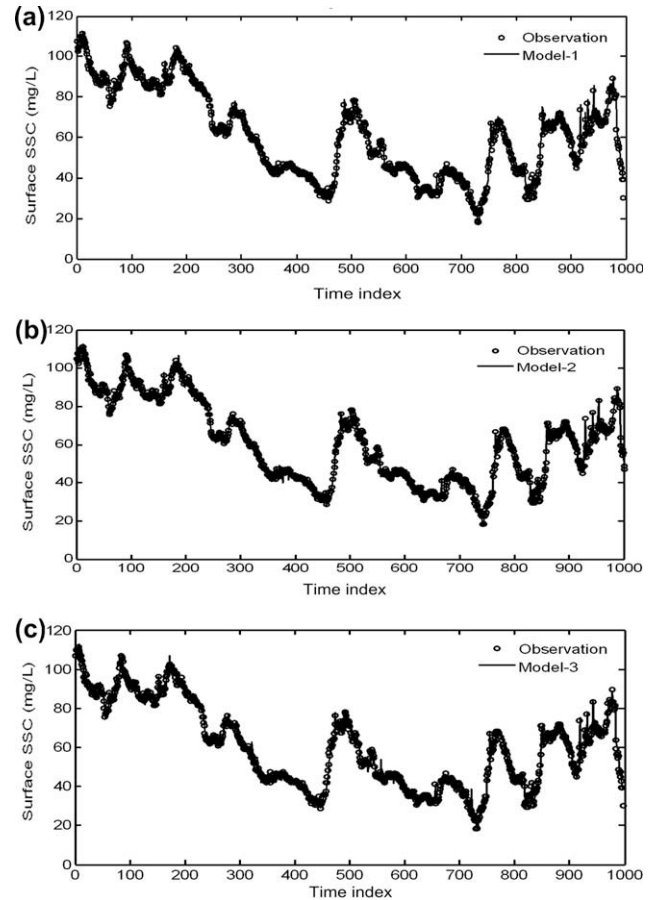


Fig. 6. Predicted and measured time series plots for surface suspended solid concentration (SSC) using: (a) Model 1, (b) Model 2, (c) Model 3.

based on the inputs of the previous surface SSC (at $k - 1$ time level) and one of the chosen variables from wind speed, flow velocity, and flow direction are developed respectively as Model 1, Model 2, and Model 3 (see Table 1). In addition, the Model 10 can be used to predict the current surface SSC using surface SSC data from two previous time levels (i.e. $k - 1$ and $k - 2$ time levels) at occasions the data of wind speed, flow velocity, and flow direction are not available. For the SSC at other layers, we also develop six models (named as Model 4, Model 5, Model 6, Model 7, Model 8, and Model 9) to predict the SSC values at middle and bottom layers using only inputs from surface data.

For the Model 1 with inputs of previous SSC and wind speed, the Kriging contour map shown in Fig. 2a demonstrates the strong relationship between $SSC(k - 1)$ ($k - 1$ time level) and $SSC(k)$ (k time level or current time level). Contour results generally can be divided into three different sets as Low, Medium, and High. When $SSC(k - 1)$ increases, $SSC(k)$ increases. It is also shown that when wind speed(k) is High, $SSC(k)$ is High. When wind speed(k) is Low or Medium, $SSC(k)$ is Low or Medium, respectively. These rules are similar to those proposed in the fuzzy logic sets by Zadeh (1965). This contour plot shows the positive correlations between these variables.

Examining the effect of current flow velocity on the surface SSC as considered in Model 2, we notice from Fig. 2b that no apparent positive correlation between flow velocity(k) and $SSC(k)$ can be concluded. An increase in SSC is seen in lower flow velocity values. This may be a combined result of sediment settling and reduced sediments transported out from the station L006. The data revealing the transport of sediment from a certain flow direction to

station L006 are presented in Fig. 2c for the development of Model 3. The contour plot shows that there is an increase in surface $SSC(k)$ value in the $120 - 180^\circ$ band of the surface layer at L006. The 120 to 180° band (counterclockwise from the east direction) corresponds to the flow from the south-east to the flow from the east direction. Consequently, the flows that move within the range from the south-east to the east directions carry more SSC as compared to SSC from other directions. The results from Model 1, Model 2 and Model 3 indicate that wind speed has a more dominating effect on the prediction of surface SSC than flow velocity and flow direction.

For the Model 4 considering the inputs of wind speed and surface SSC to the prediction of middle-layer SSC, the contour plot in Fig. 3a, as expected, shows a strong relationship between surface $SSC(k)$ and middle-layer $SSC(k)$. The direct wind effect is not significant. However, as described above, wind affects strongly the surface SSC, therefore, indirectly impacts the change of SSC in the middle layer through the change of the surface SSC. The results in Fig. 3b used for the development of Model 5 suggest that the surface flow velocity also has less influence on the middle-layer SSC than the surface SSC. The surface SSC is the major input variable that affects the prediction of the middle-layer SSC. For the effect of flow direction on the middle-layer SSC (Model 6), the contour map in Fig. 3c indicate that sediments are generally transported to the middle layer from band of 0 to 100° (flow from west to flow from south-east) direction. The results in Figs. 2c and 3c show that the surface $SSC(k)$ and middle-layer $SSC(k)$ are affected by different fluid flow directions at L006. For the prediction of bottom-layer SSC using Model 7, Model 8, and Model 9, surface $SSC(k)$

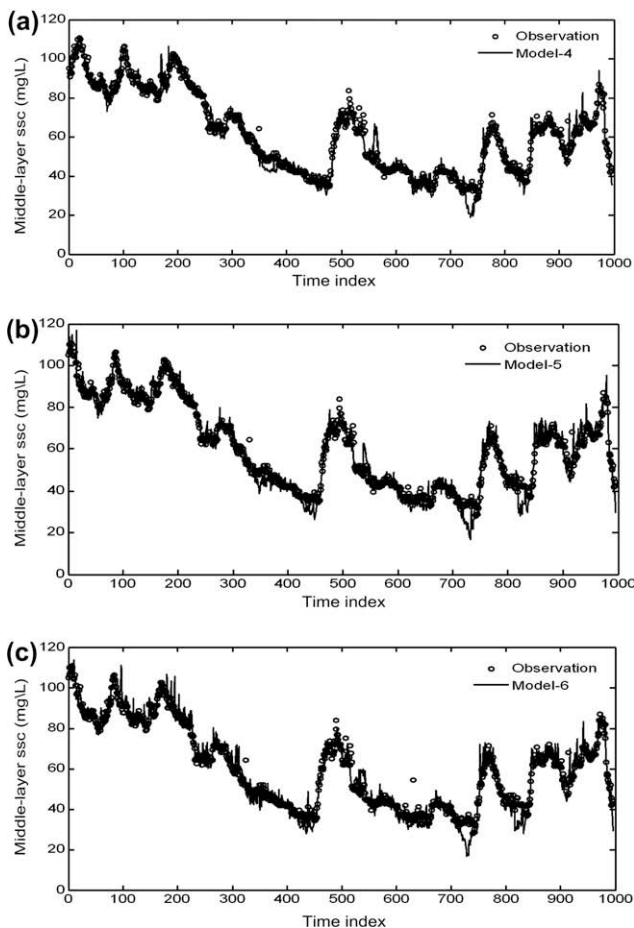


Fig. 7. Predicted and measured time series plots for middle-layer suspended solid concentration (SSC) using: (a) Model 4, (b) Model 5, (c) Model 6.

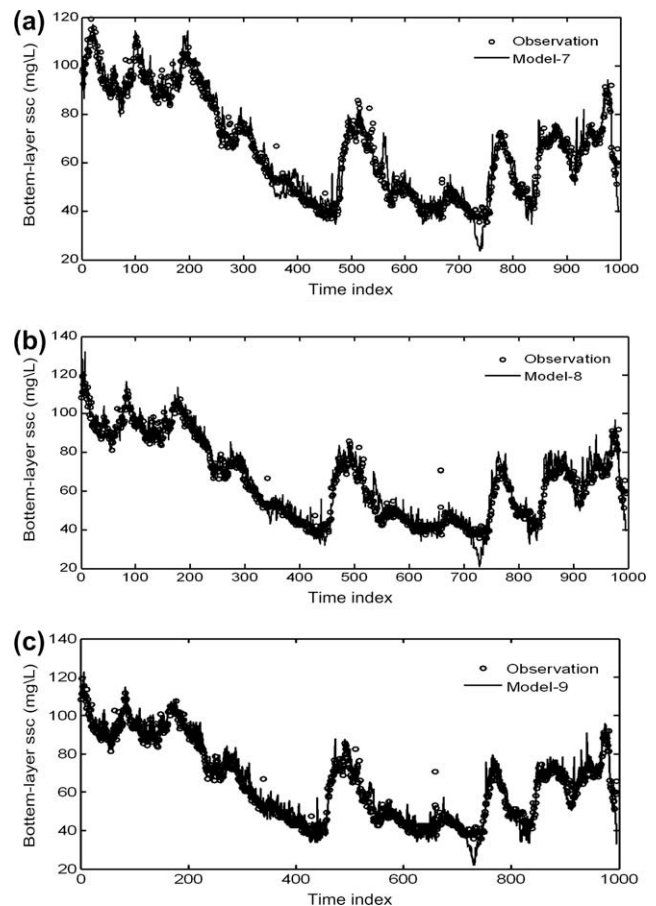


Fig. 8. Predicted and measured time series plots for bottom-layer suspended solid concentration (SSC) using: (a) Model 7, (b) Model 8, (c) Model 9.

is again revealed to have a greater contribution to the bottom-layer SSC(*k*) as shown in Fig. 4a–c. The surface flow velocity is not shown to have strong correlation with the bottom-layer SSC. For the effect of the flow direction, the contour plot in Fig. 4c shows that the bottom-layer SSC(*k*) is affected mostly by the south-east flow to north-east flow (150–230°).

A Contour map for Model 10 is constructed in Fig. 5 using the surface SSC(*k*) and two previous surface SSCs, i.e. SSC(*k* – 2) and SSC(*k* – 1). This map shows obviously that there is a strong relationship among the data of surface SSC(*k*), SSC(*k* – 1), and SSC(*k* – 2). Also, while the values of surface SSC(*k* – 2) and SSC(*k* – 1) increase, surface SSC(*k*) increases. This indicates that the autocorrelation of SSC(*k*) either with lag-1 data of SSC(*k* – 1) or with lag-2 data of SSC(*k* – 2) is strong.

The time series plots showing the comparisons of measured surface SSCs and the predicted values using Model 1, Model 2, and Model 3 for the data set selected for prediction are presented in Fig. 6a–c, respectively. The time series data selected for prediction include 1000 data points and the time index shown along the horizontal coordinate represents time with each unit being equal to 15 min. From Fig. 6a–c, it is noted that the predicted values follow the recorded data with great consistency. Mean relative error is 3.03% and root mean squared error is 3 mg/L for Model 1. Also, the coefficient of efficiency, CE, showing the consistency between measured and predicted data, is 0.98. The CE is defined as $CE = 1 - (\text{mean square errors} / \text{variance of observation})$. The good agreement between observation and prediction for Model 1 is also demonstrated in Fig. 10a with a plot of predicted surface SSCs with measured data following the 45° perfect model line.

The results obtained by using the Model 2 give respectively the mean relative error, root mean squared error, and coefficient of efficiency as 3.21%, 3.07 mg/L and 0.98. The consistency between observation and prediction is also shown to follow the perfect model line in Fig. 10b. When Model 3 is applied, the values of mean relative error, root mean squared error, and coefficient of efficiency are respectively 3.37%, 3.14 mg/L, and 0.98, similar to the results computed from Model 1 and Model 2. The trend of agreement between observation and prediction for Model 3 is shown in Fig. 10c. Although each model among Models 1, 2, and 3 produces similar predictions, slightly enhanced scattering data along the 45° line are shown in Fig. 10b and c when compared to the data plot in Fig. 10a. This further confirms that the correlation of SSC(*k*) and wind speed(*k*) is greater than the correlation between SSC(*k*) and flow velocity(*k*) or flow direction(*k*). Considering the convenience of the inputs of the affecting variables and the accuracy of the model prediction, Model 1 can be served as a practical and effective model for estimating surface SSC.

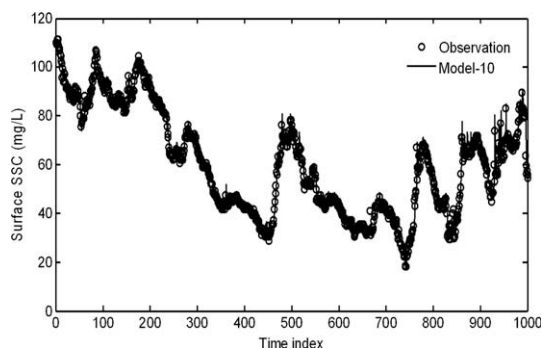


Fig. 9. Predicted and measured time series plots for surface suspended solid concentration (SSC) using Model 10.

In principle, measurements in the middle and bottom layers are relatively difficult and not cost-effective when compared to the surface measurements. Extending the measurements of surface SSC to predict middle or bottom-layer SSC can be practically important. Models 4–6 are developed to predict the middle-layer SSC(*k*) and Models 7–9 can be used to predict the bottom-layer SSC(*k*) by using wind speed(*k*), flow velocity(*k*), flow direction(*k*), and surface SSC(*k*) as inputs. For the estimation of middle-layer SSC, the predicted time series results using Model 4, Model 5, and Model 6 are given in Fig. 7a–c, respectively, whereas the corresponding perfect model line plots are shown in Fig. 11a–c. The comparison plots for the predicted bottom-layer SSCs using Model 7, Model 8, and Model 9 are shown respectively in Fig. 8a–c and in Fig. 12a–c. Examining the results shown in Figs. 7 and 8, it is noted that the middle-layer SSC(*k*) can be predicted with less error than the bottom-layer SSC(*k*). Greater deviations, when comparing to the recorded data, are noticed in predicted values in Fig. 8 than those in Fig. 7. In general, predictions of middle-layer SSC(*k*) and

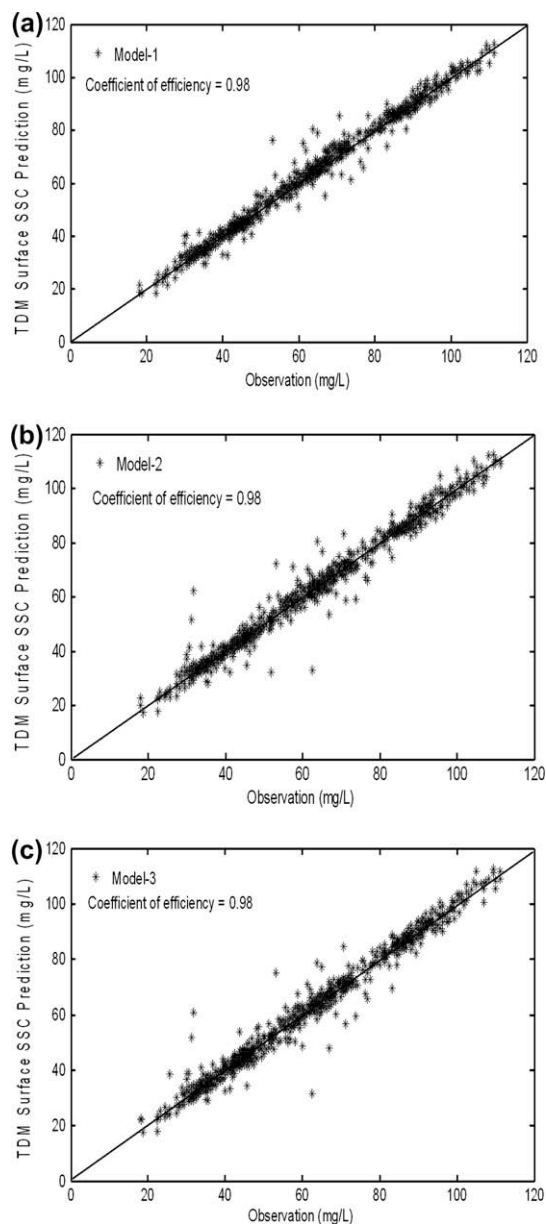


Fig. 10. Comparisons of observed and predicted surface suspended solid concentration (SSC) using: (a) Model 1, (b) Model 2, (c) Model 3.

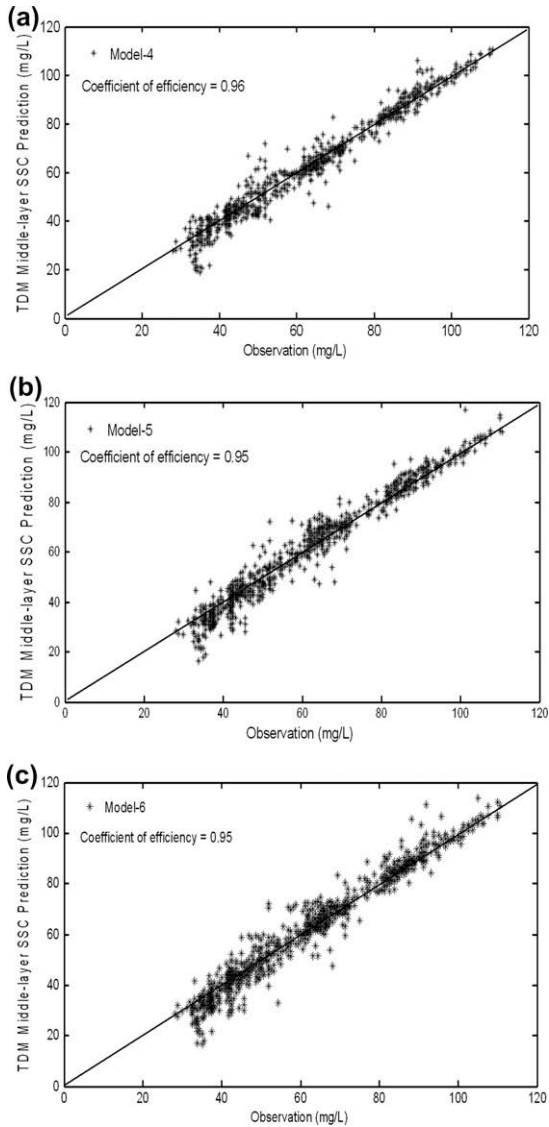


Fig. 11. Comparisons of observed and predicted middle-layer suspended solid concentration (SSC) using: (a) Model 4, (b) Model 5, (c) Model 6.

bottom-layer $SSC(k)$ are in the acceptable error range for engineering applications.

Model 10 is a model for predicting surface $SSC(k)$ using two antecedent values, i.e. $SSC(k-1)$ and $SSC(k-2)$, as inputs. The predicted time variations of surface SSC using Model 10 are presented in Fig. 9 and the perfect model line plot with the comparisons to the measured data is shown in Fig. 13. The respective mean relative error, root mean squared error, and coefficient of efficiency of 3.73%, 3.46 mg/L and 0.97 suggest that Model 10 can also be served as an appropriate predictive model for estimating surface SSC.

Overall, the mean relative errors of the presented 10 models in this study are below 7%. Also, the coefficient of efficiency that shows the consistency between observation and the prediction of the models is above 0.92. This study suggests that there is a strong and positive correlation between $SSC(k-1)$ and $SSC(k)$. Wind speed is also shown to have a more dominating effect on the prediction of surface $SSC(k)$ than variables of flow velocity(k) and flow direction(k). It is also found that the middle-layer or bottom-layer SSC can be reasonably predicted using the inputs of surface SSC and other hydrodynamic variables.

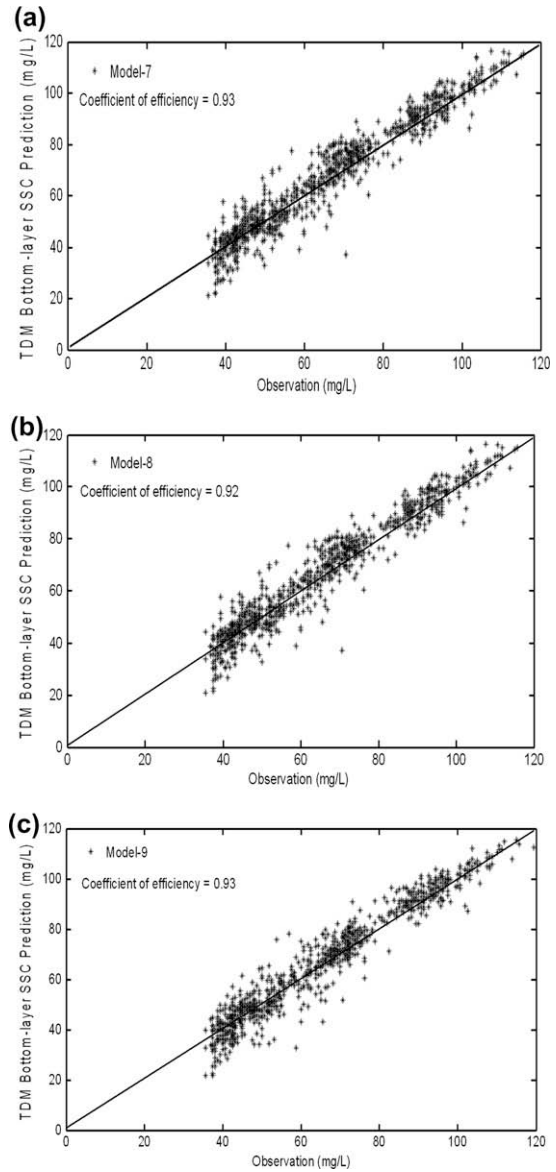


Fig. 12. Comparisons of observed and predicted bottom-layer suspended solid concentration (SSC) using: (a) Model 7, (b) Model 8, (c) Model 9.

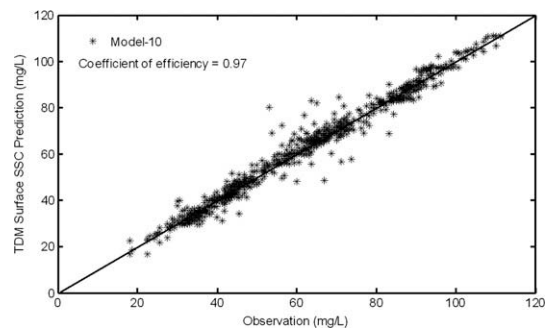


Fig. 13. Comparisons of observed and predicted surface suspended solid concentration (SSC) using Model 10.

5. Conclusions

The application of TDM approach for the development of predictive models for the determination of time variation of

suspended solid concentration either at the surface, middle or bottom-layers at a location in Lake Okeechobee, Florida is presented in this paper. The recorded wind speed, flow velocity, flow direction and SSC data at station L006 in this lake are used for this study. The data are divided into two parts for the development of the models. 3500 data for training (calibration) and 1000 data for prediction (testing or validation) are assigned. Contour maps are established from the training data and 1000 testing data are predicted by Kriging technique. Mean relative error, root mean squared error and coefficient of efficiency are obtained for the developed 10 TDMs. It occurs that wind speed has the greatest influence on SSC. The wind speed associated Model 1 has a considerable advantage when compared to other models due to the greater availability of the measured wind data. Predicted results of these 10 TDMs are presented in graphs as time series and perfect model line for comparisons with measured data. In general, the mean relative error is below 7%, and coefficient of efficiency is above 0.92 for models described in this paper. These results show that all 10 TDMs work efficiently. Depending on the availability of the recorded data of the influencing variables, appropriate predictive models as presented in this study can be applied to provide reliable estimation of the SSC in the region near the station L006. Similar methodology can also be extended to develop models for other locations in Lake Okeechobee.

References

- Altunkaynak, A., 2005. Significant wave height prediction by using a spatial model. *Ocean Eng.* 32 (8-9), 924–936.
- Altunkaynak, A., 2009. Streamflow estimation using optimal regional dependency function. *Hydrol. Process.* 23, 3525–3533.
- Altunkaynak, A., Özger, M., Şen, Z., 2003. Triple diagram model of level fluctuations in Lake Van, Turkey. *Hydrol. Earth Syst. Sci.* 7 (2), 235–244.
- Cressie, N.A.C., 1993. *Statistics for Spatial Data*. John Wiley and Sons, New York.
- Isaaks, E.H., Srivastava, R.M., 1989. *An Introduction to Applied Geostatistics*. Oxford University Press, New York.
- James, R.T., Smith, V.H., Jones, B.L., 1995. Historical trends in the Lake Okeechobee ecosystem, III. Water quality. *Arch. Hydrobiol./Suppl. (Monographische Beitrage)* 107, 49–69.
- Jin, K.R., Ji, Z.G., 2004. Case study: modeling of sediment transport and wind-wave impact in Lake Okeechobee. *J. Hydraul. Eng.* 130 (11), 1055–1067.
- Jin, K.R., Ji, Z.G., Hamrick, J.H., 2002. Modeling winter circulation in Lake Okeechobee. *J. Waterw., Port, Coastal, Ocean Eng.* 128 (3), 114–125.
- Journel, A.G., Huijbregts, Ch.J., 1978. *Mining Geostatistic*. Academic Press, London.
- Krige, D.G., 1951. A statistical approach to some basic mine evaluation problems on the Witwatersrand. *J. Chim. Min. Soc. South-Africa* 52, 119–139.
- Liu, X., Huang, W., 2009. Modeling sediment resuspension and transport induced by storm wind in Apalachicola Bay, USA. *Environ. Modell. Software* 24, 1302–1313.
- Matheron, G., 1963. Principles of geostatistics. *Econ. Geol.* 58, 1246–1266.
- Matias, J.M., Vaamonde, A., Taboada, J., Gonzalez-Manteiga, W., 2004. Comparison of Kriging and neural networks with application to the exploitation of a slate mine. *J. Math. Geol.* 36 (4), 463–486.
- Ozger, M., Sen, Z., 2007. Triple diagram method for the prediction of wave height and period. *Ocean Eng.* 34 (7), 1060–1068.
- Öztürk, C.A., Nasuf, E., 2002. Geostatistical assessment of rock zones for tunneling. *Tunn. Underground Space Technol.* 17 (3), 275–285.
- Reddy, K.R., 1991. Lake Okeechobee phosphorus dynamics study, vol. III. Biogeochemical Processes in the Sediments. SFWMD Report (C-91-2393).
- Reedy, K.R., White, J.R., Fisher, M.M., Pant, H.K., Wang, Y., Grace, K., Harris, W.G., 2002. Potential Impacts of Sediment Dredging on Internal Phosphorus Load in Lake Okeechobee, Summary Report, Soil and Water Science Department, University of Florida.
- Şen, Z., 1989. Cumulative semivariogram model of regionalized variable. *Math. Geol.* 21, 891–903.
- Şen, Z., Altunkaynak, A., Özger, M., 2004. El Niño Southern Oscillation (ENSO) templates and streamflow prediction. *J. Hydrol. Eng.* 9 (5), 368–374.
- South Florida Water Management District (2007). Lake Okeechobee Protection Program. Lake Okeechobee Protection Plan Evaluation Report.
- Subyani, A.M., 1997. *Geostatistical Analysis of Precipitation in Southwest Saudi Arabia*. Ph.D. Thesis, Colorado State University.
- Wang, K.H., 2000a. Hydrodynamic data collection for Lake Okeechobee Hydrodynamic Model validation, vol. 1. Sample Hydrodynamic and Suspended Sediment Concentration Data. University of Houston, Houston, TX.
- Wang, K.H., 2000b. Hydrodynamic data collection for Lake Okeechobee Hydrodynamic Model validation, vol. 2. Data analysis. University of Houston, Houston, TX.
- Wang, K.H., Jin, K.R., Tehrani, M., 2003. Field measurement of flow velocities, suspended solids concentrations, and temperatures in Lake Okeechobee. *J. Am. Water Resour. Assoc.* 39 (2), 441–456 (April).
- Zadeh, L.A., 1965. Fuzzy sets. *Inf. Control* 8, 338–353.